Environ. Sci. Technol. **2009,** *43,* 4068–4075

Mechanistic and Kinetic Studies on the Homogeneous Gas-Phase Formation of PCDD/Fs from 2,4,5-Trichlorophenol

XIAOHUI QU,[†] HUI WANG,[‡] QINGZHU ZHANG,*[,†] XIANGYAN SHI,[†] FEI XU,[†] AND WENXING WANG[†]

Environment Research Institute, Shandong University, Jinan 250100, P. R. China, and Department of Environmental Science and Engineering, Tsinghua University, Beijing 100084, P. R. China

Received October 8, 2008. Revised manuscript received March 12, 2009. Accepted April 20, 2009.

An understanding of the reaction mechanism of polychlorinated dibenzo-*p*-dioxins and dibenzofurans (PCDD/Fs) formation is crucial for any attempt to prevent PCDD/Fs formation. Among the polychlorophenols, 2,4,5-trichlorophenol (2,4,5-TCP) has the minimum number of Cl atoms needed to form 2,3,7,8-tetrachlorinated dibenzo-*p*-dioxin (2,3,7,8-TeCDD), which is the most toxic among all 210 PCDD/F isomers. Experiments on the formation of PCDD/Fs from the 2,4,5-TCP precursor have been hindered by the strong toxicity of 2,3,7,8-TeCDD. In this work, we carried out molecular orbital theory calculations for the homogeneous gas-phase formation of PCDD/Fs from the 2,4,5-TCP precursor. Several energetically favorable formation pathways were revealed for the first time. The rate constants of crucial elementary steps were deduced over a wide temperature range of 600∼1200 K, using canonical variational transition state theory with small curvature tunneling contribution. The rate temperature formulas were fitted. This study shows that the formation of polychlorinated dibenzo-*p*-dioxins (PCDDs) from the 2,4,5-TCP precursor is preferred over the formation of polychlorinated dibenzofurans (PCDFs). The chlorine substitution pattern has a significant effect on the dimerization of chlorophenoxy radicals.

1. Introduction

Polychlorinated dibenzo-*p*-dioxins (PCDDs) and dibenzofurans (PCDFs) are notorious for their acute and chronic toxicity and their carcinogenic, teratogenic, and mutagenic effects (*1*). PCDD/Fs were never intentionally synthesized for commercial purposes but are formed as byproducts from the synthesis of chlorinated aromatic compounds during bleach processes in the pulp and paper industries and combustion (natural and anthropogenic) processes and even as microbial byproducts in activated sludge basins fed with chlorophenol-containing waste (*2*−*4*). In particular, a large quantity of PCDD/Fs is emitted from the combustion of waste materials in municipal incinerators (*5*−*7*). Reports of PCDD/F emissions from municipal waste incinerators have caused much public alarm and have led to severe difficulties in constructing municipal and hazardous waste incinerators.

Despite many studies, the origin of PCDD/Fs emitted from waste incinerators continues to be a cause of considerable controversy (*8*−*10*). It is now known that the potential contributions of the gas-phase pathways to PCDD/Fs formation were underestimated by the reaction kinetic model proposed by Shaub and Tsang (*10*−*12*). The homogeneous gas-phase formation of PCDD/Fs from chlorophenol precursors was suggested to make a significant contribution to the observed PCDD/F yields in full-scale incinerators (*13*−*15*). Detailed insight into the mechanism and kinetic properties is a prerequisite for understanding the formation of PCDD/Fs. In a previous contribution from this laboratory (*16*), we have investigated the formation of PCDD/Fs from the monochlorophenol precursor, 2-chlorophenol (2-CP). As part of our ongoing work in the field, this paper presents mechanistic and kinetic studies on the homogeneous gas-phase formation of PCDD/Fs from the more highly chlorinated phenols, 2,4,5-trichlorophenol (2,4,5-TCP), and compares the formation mechanism of PCDD/Fs from the 2,4,5-TCP precursor to the formation mechanism of PCDD/Fs from the 2-CP precursor.

There are four reasons for initiating this work. First, it was suspected that an increasing degree of chlorine substitution of the precursor chlorophenols not only had an effect on the reactivity of chlorophenols, but also had an effect on the resulting PCDD/PCDF ratio (*17*). Second, trichlorophenols (TCPs) are manufactured for commercial use as biocides, disinfectants, wood preservatives, impregnating agents, paint components, cooling agents, and chemicals for processing of paper pulp and leather. The concentrations of 2,4,5-TCP were reported to be 0.1 μg/Nm^3 and 11.5 ng/g at the furnace outlets and in fly ash samples of municipal waste incinerators (*18*). The concentration of 2,4,5-TCP in the urine of the incineration workers was found to be significantly higher than the corresponding values in people who had no known occupational contact to the substances that are thought to be produced in garbage incineration (1.2 versus 0.8 μg/l) (*19*). Third, among the polychlorophenols, 2,4,5-TCP has the minimum number of Cl atoms to form 2,3,7,8-TeCDD, which is the most toxic among all of the 210 PCDD/F isomers (*20*). Experiments on the formation of PCDD/Fs from 2,4,5-TCP are dangerous because of the high toxicity of 2,3,7,8-TeCDD. In such a situation, quantum chemical calculation provides a safe alternative to studying these highly toxic compounds. Only one ab initio study is on record for the formation mechanism of PCDDs from 2,4,5-TCP (*21*). However, the formation of PCDDs via the dimerization of chlorophenoxy radicals (CPRs), which was recently suggested to be the major pathway in the homogeneous gas-phase formation of PCDD/Fs from chlorophenol precursors (*10*−*13*), was not investigated in this ab initio study (*21*). Furthermore, the formation of PCDFs from the 2,4,5-TCP precursor has not been studied (*21*). Fourth, the kinetic models that account for the contribution of the gaseous route in the production of PCDD/Fs in combustion processes use the rate constants of the elementary reactions (*11*). Becasue of the absence of direct experimental and theoretical values, the rate constants of many elementary steps were assigned to be the values reported in the literature for analogous reactions (*11, 12*). However, where there are uncertainties, the numerical values have been adjusted somewhat to bias the mechanism in favor of PCDD/Fs formation, i.e., worst case modeling (*11, 12*).

* Corresponding author fax: 86-531-8836 1990; e-mail: zqz@sdu.edu.cn.
[†] Shandong University.
[‡] Tsinghua University.

10.1021/es802835e CCC: $40.75
Published on Web 05/04/2009

2. Computational Methods

By means of the Gaussian 03 programs (*22*), high-accuracy molecular orbital calculations were carried out for the homogeneous gas-phase formation of PCDD/Fs from the 2,4,5-TCP precursor. The choice of computational levels and basis sets requires a compromise between accuracy and computational time. The geometrical parameters of reactants, transition states, intermediates, and products were optimized at the MPWB1K/6-31+G(d,p) level. The MPWB1K method is a hybrid density functional theory (HDFT) model with excellent performance for thermochemistry, thermochemical kinetics, hydrogen bonding, and weak interactions (*23*). The vibrational frequencies were also calculated at the same level in order to determine the nature of the stationary points, zero-point energy (ZPE), and thermal contributions to the free energy of activation. The minimum energy paths (MEPs) were obtained in mass-weighted Cartesian coordinates. The force constant matrices of the stationary points and selected nonstationary points near the transition state along the MEPs were also calculated in order to do the following kinetic calculations. The single-point energy calculations were carried out at the MPWB1K/6-311+G(3df,2p) level. The kinetic calculations are most sensitive to the energies. The reliability of the MPWB1K/6-311+G(3df,2p) level for the potential barriers was clarified in our recent study (*16*) on the formation of PCDD/Fs from the 2-CP precursor. The profiles of the potential energy surface were constructed at the MPWB1K/6-311+G(3df,2p)//MPWB1K/6-31+G(d,p) level, including ZPE correction.

By means of the Polyrate 9.3 program (*24*), direct dynamics calculations were carried out using the canonical variational transition state theory (CVT). Canonical variational transition state theory (*25*−*27*) is based on the idea of varying the dividing surface along a reference path to minimize the rate constant. The CVT rate constant for temperature T is given by

$$k^{\mathrm{CVT}}(T) = \min_{s} k^{\mathrm{GT}}(T,s) \tag{1}$$

where

$$k^{\mathrm{GT}}(T,s) = \frac{\sigma k_{\mathrm{B}} T}{h} \frac{Q^{\mathrm{GT}}(T,s)}{\Phi^{\mathrm{R}}(T)} e^{-V_{\mathrm{MEP}}(s)/k_{\mathrm{B}}T} \tag{2}$$

where, $k^{\mathrm{GT}}(T, s)$ is the generalized transition state theory rate constant at the dividing surface s, σ is the symmetry factor accounting for the possibility of more than one symmetry-related reaction path, k_{B} is Boltzmann's constant, h is Planck's constant, $\Phi^{\mathrm{R}}(T)$ is the reactant partition function per unit volume (excluding symmetry numbers for rotation), and $Q^{\mathrm{GT}}(T, s)$ is the partition function of a generalized transition state at s with a local zero of energy at $V_{\mathrm{MEP}}(s)$ and with all rotational symmetry numbers set to unity. The level of the tunneling calculation is the small curvature tunneling (SCT) (*28*) method, based on the centrifugal dominant small curvature semiclassical adiabatic ground state (CD-SCSAG) approximation. The rotational partition functions were calculated classically, and the vibrational modes were treated as quantum-mechanically separable harmonic oscillators. The error of the kinetic calculation may be mainly from the small curvature tunneling (SCT) method, especially for the heavy−light−heavy (HLH) mass combination reactions. The large curvature tunneling approximation may be especially desirable to model this kind of reaction in detail. Methods for large curvature cases have been developed (*29*), but they require more information about the potential energy surface than was determined in the present study. So, the SCT approximation becomes an alternative to the large curvature approximation. The new CD-SCSAG approximation for small curvature tunneling is an improvement over the original SCSAG method in that it accounts for the effect of mode−mode coupling on the extent of corner cutting through each vibrational degree of freedom, orthogonal to the reaction path (*30*). Furthermore, previous studies (*31, 32*) show that the tunneling correction plays an important role, mainly in a low-temperature range for the calculation of the rate constants. Fortunately, the rate constants were calculated over a high-temperature range (600∼1200 K) in this work. The error from the tunneling calculation does not significantly influence the reliability of our results.

3. Results and Discussion

The first step in this study was to identify the level of theoretical approximation that was not only able to produce accurate results but was also computationally feasible and economical for currently available hardware and software. The geometric parameters and the vibrational frequencies of phenol, chlorobenzene, and 2,3,7,8-TeCDD were calculated at the MPWB1K/6-31+G(d,p) level. The results agree well with the available experimental values (*33*−*36*), and the maximum relative error is less than 1.4% for the geometrical parameters and less than 8.0% for the vibrational frequencies. From this results, we infer that the same accuracy can be expected for the species involved in the formation of PCDD/Fs from the 2,4,5-TCP precursor. Furthermore, a previous study shows that MPWB1K is an excellent method for prediction of transition state geometries (*23*).

For 2,4,5-TCP, there are two geometric conformers resulting from the two main orientations of the hydroxyl-hydrogen due to the asymmetric chlorine substitutions. The conformer with the hydroxyl-hydrogen facing the closest neighboring Cl is labeled the *syn* conformer, and the other is the *anti* conformer. The *syn* conformer is more stable by 3.24 kcal/mol than the corresponding *anti* form. So throughout this paper, 2,4,5-TCP denotes the *syn* conformer.

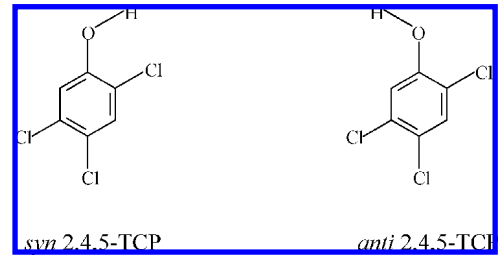

syn 2,4,5-TCP *anti* 2,4,5-TCP

3.1. Formation of 2,4,5-Trichlorophenoxy Radicals.

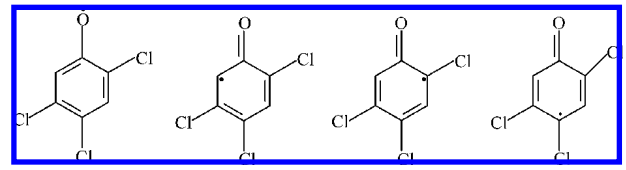

The chlorophenoxy radical (CPR), in which the electrons are delocalized, is a hybrid of one oxygen-centered and three carbon-centered radicals (2 *ortho* and 1 *para* carbon sites). The resonance structures provide about 16 kcal/mol of resonance stabilization energy for phenoxy radicals (*37*). The resonance stabilization energy of CPR should be approximately identical to the value of phenoxy radical. The high resonance stabilization energy means that CPRs could build up sufficient concentrations to enable self-condensation to occur. Recent works (*13, 38*) have shown that the dimerization of CPRs is the major pathway in the homogeneous gas-phase formation of PCDD/Fs. Thus, we first studied the formation of 2,4,5-trichlorophenoxy radicals (2,4,5-TCPRs). In municipal waste incinerators, 2,4,5-TCPRs can be formed through

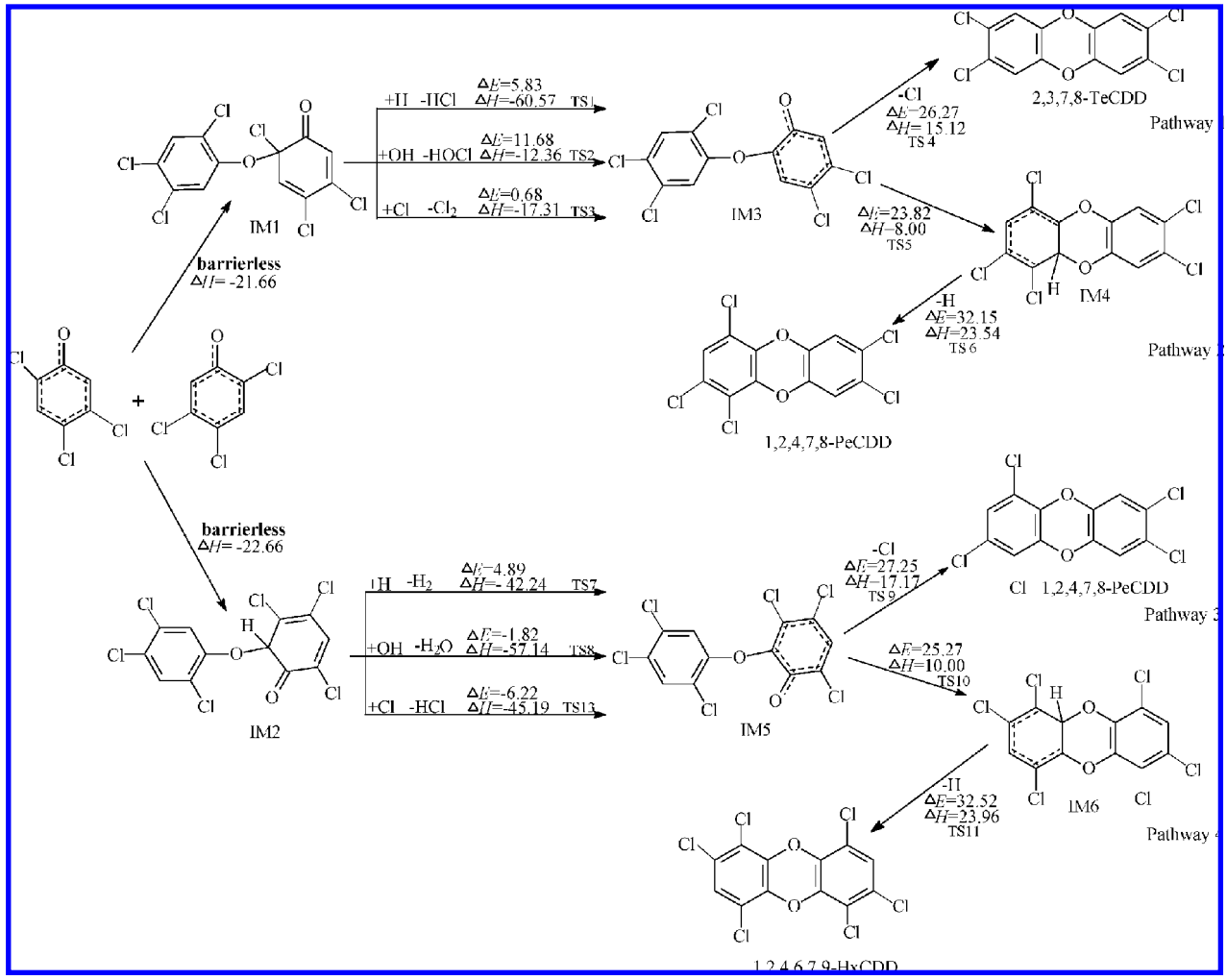

FIGURE 1. Formation routes of PCDDs from the 2,4,5-TCP precursor. Δ*H* is calculated at 0 K.

loss>of phenolic-hydrogen via unimolecular, bimolecular, or possibly other low-energy pathways (including heterogeneous reactions). The unimolecular reaction includes the decomposition of 2,4,5-TCP with cleavage of the O−H bond. The profile of the potential energy surface was scanned by varying the O−H bond length. We found no energy exceeding the O−H bond dissociation threshold along the reaction coordinate. This shows that there is no transition state in the decomposition process.

$$\text{2,4,5-TCP} \rightarrow \text{2,4,5-TCPR} + \text{H} \qquad \Delta H = 85.37 \text{ kcal/mol}$$

In the combustion environment, abundant active radicals will greatly facilitate the formation of 2,4,5-TCPRs. The bimolecular reactions include attack by H or Cl under pyrolytic conditions and by H, OH, O (^{3}P), or Cl under high-temperature oxidative conditions. Studies show that the formation of 2,4,5-TCPRs from the bimolecular reactions of 2,4,5-TCP with H, OH, O (^{3}P), and Cl proceeds via a direct phenolic hydrogen abstraction mechanism. The potential barriers (Δ*E*) and the reaction enthalpies (Δ*H*, 0 K) were calculated at the MPWB1K/6-311+G(3df,2p)//MPWB1K/6-31+G(d,p) level. The reaction enthalpies at 600 and 1000 K are presented in the Supporting Information. Particularly, for the phenolic hydrogen abstraction from 2,4,5-TCP by Cl, the energy of the transition state without ZPE (zero-point energy) correction is 0.94 kcal/mol higher than the total energy of the original reactants (2,4,5-TCP and Cl). However, the energy of the transition state, including ZPE, is 1.93 kcal/mol lower than the total energy of the original reactants. This is because the zero-point energy of the transition state for the phenolic hydrogen abstraction from 2,4,5-TCP by Cl is 2.87 kcal/mol lower than that of 2,4,5-TCP.

$$\text{2,4,5-TCP} + \text{H} \rightarrow \text{2,4,5-TCPR} + \text{H}_2$$
$$\Delta E = 13.96 \text{ kcal/mol} \quad \Delta H = -12.56 \text{ kcal/mol}$$
$$\text{2,4,5-TCP} + \text{OH} \rightarrow \text{2,4,5-TCPR} + \text{H}_2\text{O}$$
$$\Delta E = 3.23 \text{ kcal/mol} \quad \Delta H = -27.46 \text{ kcal/mol}$$
$$\text{2,4,5-TCP} + \text{O}(^3\text{P}) \rightarrow \text{2,4,5-TCPR} + \text{OH}$$
$$\Delta E = 7.67 \text{ kcal/mol} \quad \Delta H = -11.89 \text{ kcal/mol}$$
$$\text{2,4,5-TCP} + \text{Cl} \rightarrow \text{2,4,5-TCPR} + \text{HCl}$$
$$\Delta E = -1.93 \text{ kcal/mol} \quad \Delta H = -15.51 \text{ kcal/mol}$$

The potential barriers of the phenolic hydrogen abstraction from 2,4,5-TCP are a little higher than those from 2-CP. For example, the potential barrier of 2,4,5-TCP + H → 2,4,5-TCPR + H_2 is 13.93 kcal/mol at the MPWB1K/6-311+G(3df,2p)//MPWB1K/6-31+G(d,p) level, and the value for 2-CP + H → 2-CPR + H_2 is 13.80 kcal/mol (*16*). The phenolic hydrogen abstraction from 2,4,5-TCP is a little more exothermic than the phenolic hydrogen abstraction from 2-CP. For example, the reaction of 2,4,5-CP + OH → 2-CPR + H_2O is exothermic by 27.46 kcal/mol (0 K), whereas the reaction of 2-CP + OH → 2-CPR + H_2O is exothermic by 26.91 kcal/mol (0 K) at the MPWB1K/6-311+G(3df,2p)//MPWB1K/6-31+G(d,p) level (*16*). The degree of chlorination has an effect on the potential barrier and reaction enthalpies for the phenolic hydrogen abstraction from chlorophenols.

3.2. Formation of PCDD/Fs from 2,4,5-Trichlorophenoxy Radicals. *3.2.1. Formation of PCDDs from 2,4,5-*

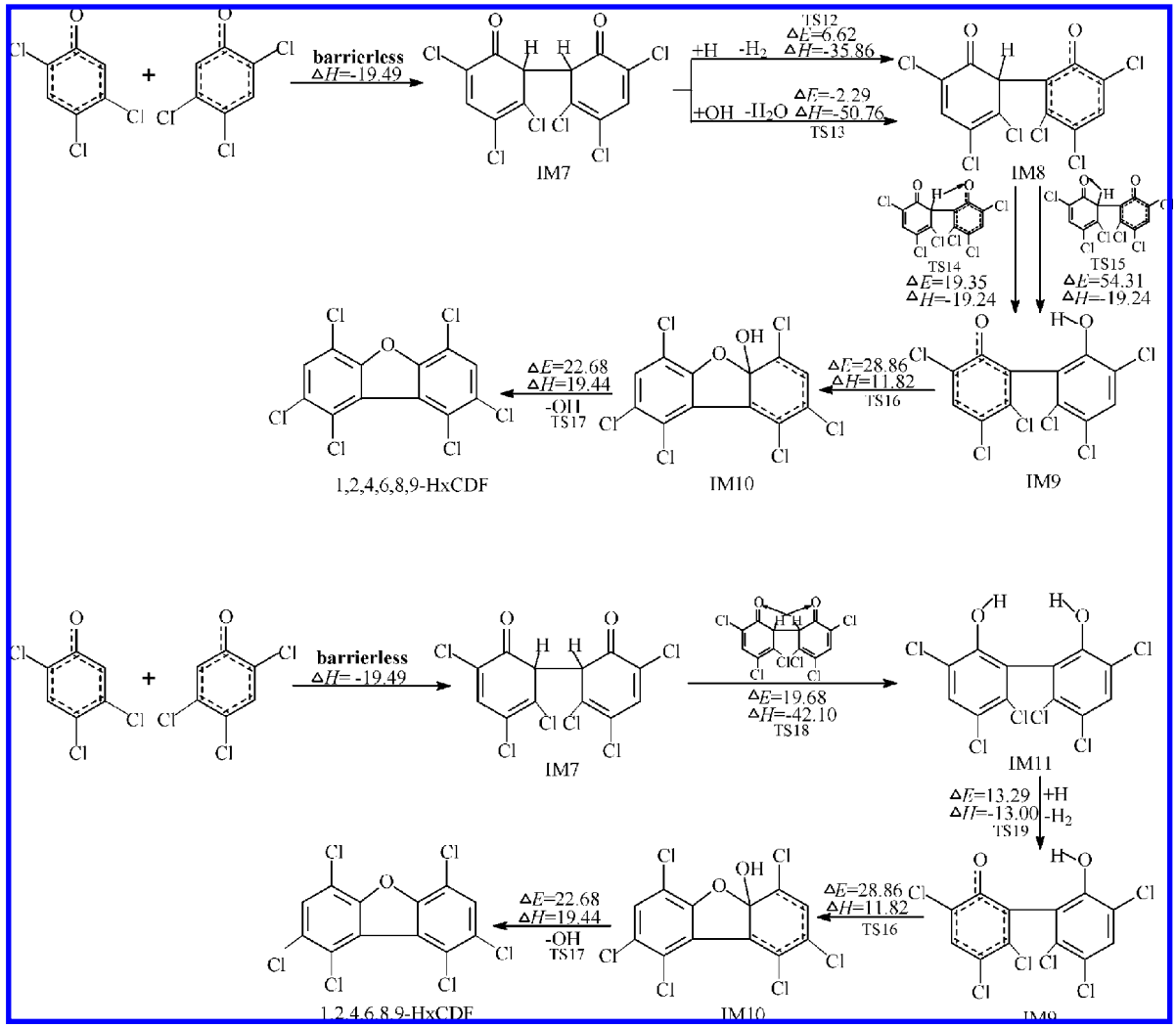

FIGURE 2. Formation routes of 1,2,4,6,8,9-H*x*CDF from the 2,4,5-TCP precursor. Δ*H* is calculated at 0 K.

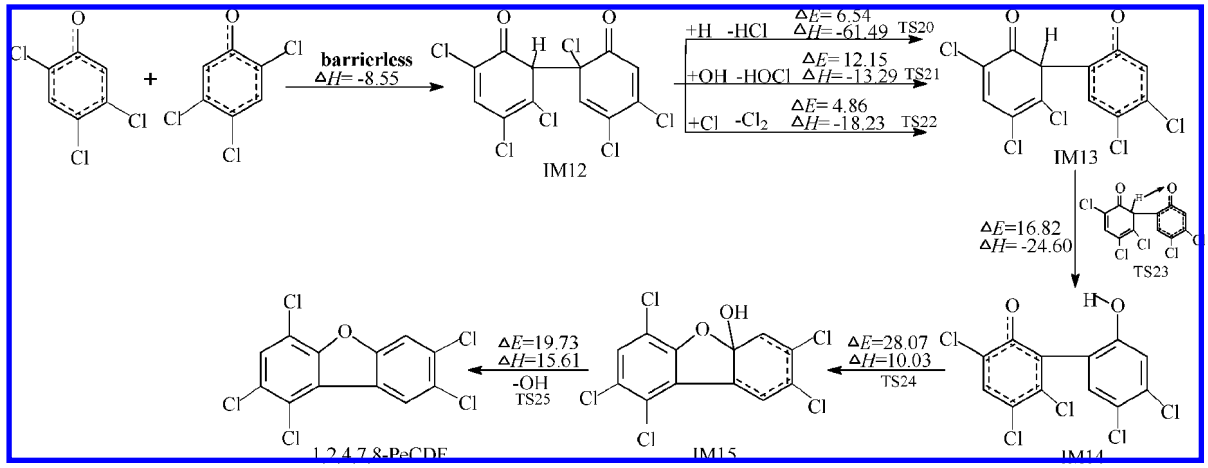

FIGURE 3. Formation route of 1,2,4,7,8-PeCDF from the 2,4,5-TCP precursor. Δ*H* is calculated at 0 K.

Trichlorophenoxy Radicals. Previous research (*39*, *40*) has shown that the formation of PCDDs can be attributed to the formation of *o*-phenoxy-phenol (POP) intermediates. There are two possible oxygen−carbon coupling modes to form POPs from the self-condensation of 2,4,5-TCPRs. Thus, two POP intermediates, denoted IM1 and IM2, were identified in this study. In order to evaluate the nature of the entrance channel for the two coupling reactions, we examined the potential along the reaction coordinate, especially to determine whether there is a well-defined transition state or the coupling proceeds via a loose transition state without a barrier. The profile of the potential energy surface was scanned against the newly formed C−O bond length. We find no energy exceeding the C−O bond dissociation threshold along the reaction coordinate. This shows that both coupling reactions appear to be barrierless.

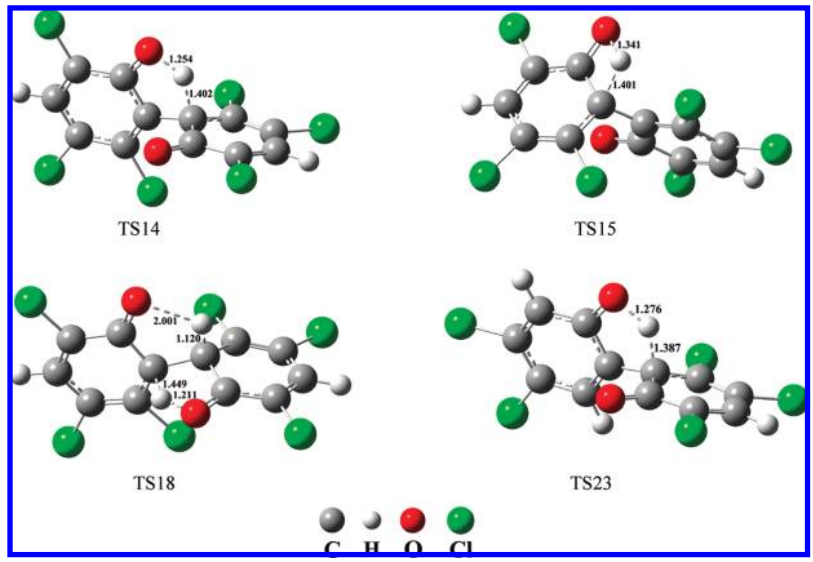

FIGURE 4. Configurations of the transition states of H-shift involved in the formation of PCDFs.

Similar to the formation of PCDDs from the 2-CP precursor (*16*), three possible PCDD congeners, 2,3,7,8-tetrachlorinated dibenzo-*p*-dioxin (2,3,7,8-TeCDD), 1,2,4,7,8-pentachlorinated dibenzo-*p*-dioxin (1,2,4,7,8-PeCDD), and 1,2,4,6,7,9-hexachlorinated dibenzo-*p*-dioxin (1,2,4,6,7,9-HxCDD), can be formed from oxidation or pyrolysis of 2,4,5-TCP (*13*−*15*). Four possible formation pathways, depicted in Figure 1, are proposed for the formation of the three dioxins in this study. The formation pathways involve four elementary processes: (1) dimerization (oxygen−carbon coupling) of 2,4,5-TCPRs, (2) Cl or H abstraction, (3) ring closure, and (4) intra-annular elimination of Cl or H. In pathway 1 and pathway 3, the ring closure and elimination of Cl occur in a one-step reaction. The dimerization of 2,4,5-TCPRs is a barrierless and strongly exothermic process. All of the Cl or H abstraction steps are highly exothermic with low-energy barriers. The ring closure process requires crossing a high barrier and is strongly endoergic, and it is the rate-determining step for pathways 1 and 3. Unimolecular elimination of H is the rate-determining step for pathway 2 and pathway 4 because of the high potential barrier, 32.15 and 32.52 kcal/mol, respectively. The thermodynamically favored routes for PCDD formation are pathways 1 and 3. So, 2,3,7,8-TeCDD and 1,2,4,7,8-PeCDD are the major PCDD products from the 2,4,5-TCP precursor. Congeners 2,3,7,8-TeCDD, 1,2,4,7,8-PeCDD, and 1,2,4,6,7,9-H*x*CDD were observed in the flue gas and fly ash samples of municipal waste incinerators (*41, 42*). Isomer fractions were reported (*41*). The mean concentrations of 2,3,7,8-TeCDD in the ambient air near municipal solid waste incinerators are 0.005 and 0.004 pg/Nm^3 (*42*) at two sampling sites located in southern Taiwan, respectively. Annual dry deposition fluxes of 2,3,7,8-TeCDD in the ambient air of the two sampling sites are 0.081 and 0.089 ng/(m^2 year) (*42*), respectively.

Comparison of the formation of PCDDs from the 2,4,5-TCP and 2-CP (*16*) precursors shows that the degree of chlorination affects each elementary step involved in the formation of PCDDs. In particular, the degree of chlorination has a significant effect on the dimerization of chlorophenoxy radicals (CPRs). The oxygen−carbon coupling of 2,4,5-TCPRs is more exothermic than the oxygen−carbon coupling of 2-CPRs. It appears that the trend toward POP formation increases with increasing degree of chlorination. (This appears to be the case on the basis of the limited number of chlorophenol isomers studied.) This is probably due to the fact that the nucleophilic attack of the phenolic oxygen atom at the second phenol is facilitated during the formation of the POP by the withdrawal of electron density from the aromatic system by the chlorine substituents.

The formation of PCDDs from the 2,4,5-TCP precursor was also studied by Okamoto (*21*). It is interesting to compare the formation mechanism of PCDDs proposed by Okamoto and us. In the mechanism proposed by Okamoto (*21*), intramolecular condensation, is the rate-determining step. The potential barriers (*21*) of the rate-determining steps are 2.574 eV for the formation of 2,3,7,8-TeCDD, 4.486 and 2.528 eV for the formation of 1,2,4,7,8-PeCDD, and 4.436 eV for the formation of 1,2,4,6,7,9-HxCDD at the B3LYP level, which are much higher than those involved in the dimerization mechanism proposed by us. This means chlorophenoxy radical−radical dimerization is indeed the preferred path.

3.2.2. Formation of PCDFs from 2,4,5-Trichlorophenoxy Radicals. The formation of PCDFs was based primarily on *ortho-ortho* coupling of chlorophenoxy radicals to form an *o,o*'-dihydroxybiphenyl (DOHB) intermediate (*38*). Similar to the formation of PCDFs from the 2-CP precursor (*16*), two possible PCDF congeners, 1,2,4,6,8,9-hexachlorinated dibenzofuran (1,2,4,6,8,9-HxCDF) and 1,2,4,7,8-pentachlorinated dibenzofuran (1,2,4,7,8-PeCDF), can be formed from the 2,4,5-TCP precursor. Two formation pathways for 1,2,4,6,8,9-H*x*CDF and one formation pathway for 1,2,4,7,8-PeCDF are proposed, as presented in Figures 2 and 3.

The first formation route for 1,2,4,6,8,9-H*x*CDF involves five elementary steps: (1) the *ortho*−*ortho* coupling of 2,4,5-TCPRs, (2) H abstraction by H atoms or OH radicals, (3) tautomerization (H-shift), (4) ring closure, and (5) elimination of OH. The *ortho*−*ortho* coupling is a barrierless and strongly exothermic process. Both H abstraction processes have low barriers and are strongly exothermic. The H-shift step could proceed via two different transition states: a five-membered ring transition state, denoted TS14, and a four-membered ring transition state, denoted TS15. The structures of TS14 and TS15 are shown in Figure 4. The energy of TS14 is 34.96 kcal/mol lower than that of TS15. Thus, the process via TS14 is energetically favorable for the H-shift step. The ring closure process requires crossing a large barrier, is strongly endoergic, and is the rate-determining step.

The second formation pathway of 1,2,4,6,8,9-H*x*CDF also involves five elementary processes: (1) dimerization of 2,4,5-TCPRs, (2) tautomerization (double H-transfer), (3) H abstraction, (4) ring closure, and (5) OH desorption. The double hydrogen atom migration to the key to oxygen atoms proceeding via the transition state TS18, whose geometrical structure is presented in Figure 4. The calculated vibrational

TABLE 1. CVT/SCT Rate Constants for the Phenolic Hydrogen Abstraction from 2,4,5-TCP along with the Available Experimental Rate Constants for the Phenolic Hydrogen Abstraction from Phenol (*44*−*46*)

reactions	*T* (K)	*k* (cm^3 $molecule^{-1}$ s^{-1})	reference
2,4,5-TCP + H → 2,4,5-TCPR + H_2	1000	1.10×10^{-14}	this study
phenol + H → phenoxy + H_2	1000	3.72×10^{-13}	ref *44*
2,4,5-TCP + OH → 2,4,5-TCPR + H_2O	1000	1.85×10^{-13}	this study
phenol + OH → phenoxy + H_2O	1000	9.48×10^{-12}	ref (*45*)
2,4,5-TCP + Cl → 2,4,5-TCPR + HCl	296	8.95×10^{-12}	this study
phenol + Cl → phenoxy + HCl	296	1.93×10^{-10}	ref *46*

TABLE 2. Arrhenius Formulas[a] for Elementary Reactions Involved in the Formation of PCDD/Fs from the 2,4,5-TCP Precursor over the Temperature Range of 600∼1200 K

reactions	Arrhenius formulas
2,4,5-TCP + H → 2,4,5-TCPR + H_2	$k(T) = (5.97 \times 10^{-12}) \exp(-6298.20/T)$
2,4,5-TCP + OH → 2,4,5-TCPR + H_2O	$k(T) = (1.51 \times 10^{-12}) \exp(-2099.61/T)$
2,4,5-TCP + O(^{3}P) → 2,4,5-TCPR + OH	$k(T) = (2.96 \times 10^{-13}) \exp(-3386.30/T)$
2,4,5-TCP + Cl → 2,4,5-TCPR + HCl	$k(T) = (4.87 \times 10^{-11}) \exp(-710.73/T)$
IM1 + OH → IM3 + HOCl	$k(T) = (1.88 \times 10^{-11}) \exp(-1461.15/T)$
IM1 + Cl → IM3 + Cl_2	$k(T) = (8.90 \times 10^{-12}) \exp(-7185.73/T)$
IM3 → 2,3,7,8-TeCDD	$k(T) = (2.34 \times 10^{11}) \exp(-13069.04/T)$
IM3 → IM4	$k(T) = (2.36 \times 10^{9}) \exp(-7389.52/T)$
IM4 → 1,2,4,7,8-PeCDD	$k(T) = (2.90 \times 10^{13}) \exp(-16719.64/T)$
IM2 + H → IM5 + H_2	$k(T) = (4.08 \times 10^{-12}) \exp(-1552.54/T)$
IM2 + OH → IM5 + H_2O	$k(T) = (3.11 \times 10^{-12}) \exp(-226.80/T)$
IM5 → 1,2,4,7,8-PeCDD	$k(T) = (5.70 \times 10^{9}) \exp(-10065.22/T)$
IM5 → IM6	$k(T) = (3.77 \times 10^{11}) \exp(-12656.49/T)$
IM6 → 1,2,4,6,7,9-H*x*CDD	$k(T) = (2.13 \times 10^{13}) \exp(-16809.22/T)$
IM7 + H → IM8 + H_2	$k(T) = (1.40 \times 10^{-11}) \exp(-1622.86/T)$
IM7 + OH → IM8 + H_2O	$k(T) = (3.37 \times 10^{-12}) \exp(18.30/T)$
IM8 → IM9 via TS14	$k(T) = (3.37 \times 10^{10}) \exp(-586.27/T)$
IM9 → IM10	$k(T) = (4.18 \times 10^{10}) \exp(-6141.44/T)$
IM10 → 1,2,4,6,8,9-H*x*CDF	$k(T) = (5.50 \times 10^{13}) \exp(-11874.30/T)$
IM7 → IM11	$k(T) = (1.86 \times 10^{9}) \exp(-1419.06/T)$
IM11 + H → IM9 + H_2	$k(T) = (6.72 \times 10^{-11}) \exp(-7238.72/T)$
IM12 + H → IM13 + HCl	$k(T) = (1.13 \times 10^{-10}) \exp(-4022.09/T)$
IM12 + OH → IM13 + HOCl	$k(T) = (8.58 \times 10^{-13}) \exp(-7098.10/T)$
IM12 + Cl → IM13 + Cl_2	$k(T) = (2.29 \times 10^{-11}) \exp(-3448.01/T)$
IM13 → IM14	$k(T) = (5.79 \times 10^{9}) \exp(-2159.64/T)$
IM14 → IM15	$k(T) = (3.27 \times 10^{12}) \exp(-14307.63/T)$
IM15 → 1,2,4,7,8-PeCDF	$k(T) = (3.23 \times 10^{13}) \exp(-10349.92T)$

[a] Units are s^{-1} and cm^3 $molecule^{-1}$ s^{-1} for unimolecular and bimolecular reactions, respectively.

frequencies contained one and only one imaginary component, 1532i cm^{-1}, confirming the first-order saddle point configuration. Similarly, an energetically feasible formation pathway, depicted in Figure 3, is proposed for 1,2,4,7,8-PeCDF. Both 1,2,4,6,8,9-HxCDF and 1,2,4,7,8-PeCDF were observed in municipal waste incinerator flue gas and fly ash samples (*41*).

Comparison of the formation of PCDFs from the 2,4,5-TCP and 2-CP (*16*) precursors shows that degree of chlorination has a significant effect on the *ortho*−*ortho* coupling of CPRs. The *ortho*−*ortho* coupling of 2,4,5-TCPRs proceeds via a barrierless process, whereas the *ortho*−*ortho* coupling of 2-CPRs requires crossing a potential barrier of 8.27 kcal/mol (*16*).

Comparison of Figures 1 and 2 shows that the preferred formation routes of PCDDs from the 2,4,5-TCP precursor involve three elementary steps, whereas the formation pathways of PCDFs involve five elementary processes. The POP intermediates, IM1 and IM2, can be regarded as prestructures for PCDDs. DOHB intermediates, IM7 and IM12, are prestructures of PCDFs. This study shows that the formation of POPs is more exoergic than the formation of DOHBs. It means that POPs are thermodynamically more stable than DOHBs. Furthermore, the rate-determining step (ring closure process) involved in the formation of PCDFs requires crossing a larger barrier than that involved in the formation of PCDDs. Thus, the formation of PCDDs is preferred over the formation of PCDFs from the 2,4,5-TCP precursor. Further direct experimental observation would be anticipated to verify the conclusion. However, this conclusion may be supported indirectly by the results of laboratory experiments: PCDDs are formed at lower temperatures than PCDFs, and PCDDs are the major dioxin products rather than PCDFs in the pyrolysis of 2-CP (*39*).

3.3. Kinetic Calculations. Canonical variational transition state theory (CVT) (*25*−*27*), with small curvature tunneling (SCT) (*28*) correction, has been successfully performed for the elementary reactions involved in the formation of PCDD/Fs from the 2-CP precursor (*16*) and is an efficient method to calculate the rate constants (*43*). In this study, we used this method to calculate the rate constants of crucial elementary reactions, especially the rate-determining steps involved in the PCDD/F formations from the 2,4,5-TCP precursor over a wide temperature range of 600∼1200 K, which covers the possible formation temperature of PCDD/Fs in municipal waste incinerators.

Because of the absence of available experimental values, it is difficult to make a direct comparison of the calculated CVT/SCT rate constants with the experimental values for all of the elementary reactions. An alternative approach to clarifying the reliability of the kinetics calculation is to compare the CVT/SCT rate constants with the available literature rate constants

for structurally similar compounds. There are no available experimental or theoretical rate constants for the phenolic hydrogen abstraction from 2,4,5-TCP. So, the calculated rate constants were compared with the literature values (*44*−*46*) for the phenolic hydrogen abstraction from phenol. As shown in Table 1, the CVT/SCT rate constants for the phenolic hydrogen abstraction from 2,4,5-TCP are over 1 order of magnitude lower than the literature values (*44*−*46*) for the corresponding phenolic hydrogen abstraction from phenol. For example, at 1000 K, our CVT/SCT value for 2,4,5-TCP + H → 2,4,5-TCPR + H_2 is 1.10×10^{-14} cm^3 $molecule^{-1}$ s^{-1}, whereas the rate constant for phenol + H → phenoxy + H_2 is 3.72×10^{-13} cm^3 $molecule^{-1}$ s^{-1} (*44*). A new study (*47*) from our group shows that the chlorine substitution in the *ortho* position increases the strength of the O−H bond in chlorophenol and decreases its reactivity. At the MPWB1K/6-311+G(3df,2p) level, the potential barrier for 2,4,5-TCP + H → 2,4,5-TCPR + H_2 is 13.96 kcal/mol, while the value for phenol + H → phenoxy + H_2 is 11.73 kcal/mol. The dissociation energies (0 K) of the O−H bonds in 2,4,5-TCP and phenol are 85.37 and 83.95 kcal/mol, respectively. Thus, our CVT/SCT rate constants for the phenolic hydrogen abstraction from 2,4,5-TCP are reasonable. In order to further check the validity of our computational scheme, we also calculated the rate constants for phenol + H → phenoxy + H_2, using canonical variational transition state theory (CVT) with small curvature tunneling (SCT) contribution. The CVT/SCT rate constants are in good agreement with the experimental values (*44*), with the maximum relative deviation less than 3 times that for phenol + H → phenoxy + H_2. For example, at 1000 K, the calculated CVT/SCT rate constant, 1.68×10^{-13} cm^3 $molecule^{-1}$ s^{-1}, perfectly matches the experimental value of 3.72×10^{-13} cm^3 $molecule^{-1}$ s^{-1} (*44*). From these good agreements, it is inferred that the same accuracy could be expected for the other crucial elementary reactions involved in the formation of PCDD/Fs from the 2,4,5-TCP precursor.

Regulatory decisions and risk analyses often rely on the use of mathematical models to predict the potential outcomes of contaminant releases to the environment. A better knowledge of the temperature dependence would be useful for the kinetic models that account for the contribution of the gaseous route in the production of PCDD/Fs in combustion processes (*11, 12*). The pre-exponential factor, activation energy, and rate constants are important input parameters in the kinetic models (*11, 12*). Thus, the calculated CVT/SCT rate constants are fitted over the temperature range of 600∼1200 K, and Arrhenius formulas are given in Table 2.

Acknowledgments

This work was supported by NSFC (National Natural Science Foundation of China, project No. 20737001, 20777047), Shandong Province Outstanding Youth Natural Science Foundation (project No. JQ200804) and the Research Fund for the Doctoral Program of Higher Education of China (project No. 200804220046). The authors thank Professor Donald G. Truhlar for providing the POLYRATE 9.3 program. The authors also thank Dr. Pamela Holt for proofreading the manuscript.

Supporting Information Available

MPWB1K/6-31+G(d,p) optimized geometries and calculated frequencies for the transition states involved in the formation of PCDD/Fs from 2,4,5-TCP as precursor and reaction enthalpies ($\triangle H$) of all of the elementary steps involved in the formation of PCDD/Fs from 2,4,5-TCP as precursor at 600 and 1000 K. This information is available free of charge via the Internet at http://pubs.acs.org.

Literature Cited

(1) Schecter, A. *Dioxin and Health*; Plenum Press: New York, 1994.

(2) Stefan, V.; Achim, Z.; Reinhard, N. Formation of polychlorinated dibenzo-*p*-dioxins and polychlorinated dibenzofurans during the photolysis of pentachlorophenol-containing water. *Environ. Sci. Technol.* **1994**, *28* (6), 1145–1149.

(3) Harris, J. C.; Anderson, P. C.; Goodwin, B. E.; Rechsteiner, C. E. *Dioxin Emissions from Combustion Sources: A Review of the Current State of Knowledge*; Final Report to American Society of Mechanical Engineers (ASME); ASME: New York, 1980.

(4) Addink, R.; Altwicker, E. R. Formation of polychlorinated dibenzo-*p*-dioxins/dibenzofurans from soot of benzene and *o*-dichlorobenzene combustion. *Environ. Sci. Technol.* **2004**, *38* (19), 5196–5200.

(5) Yasuhara, A.; Katami, T.; Okuda, T.; Ohno, N.; Adriaens, P. Formation of dioxins during the combustion of newspapers in the presence of sodium chloride and poly(vinyl chloride). *Environ. Sci. Technol.* **2001**, *35* (7), 1373–1378.

(6) Addink, R.; Govers, H. A. J.; Olie, K. Isomer distributions of polychlorinated dibenzo-*p*-dioxins/dibenzofurans formed during De Novo synthesis on incinerator fly ash. *Environ. Sci. Technol.* **1998**, *32* (13), 1888–1893.

(7) Chen, C. K.; Lin, C.; Lin, Y. C.; Lin, Y. C.; Wang, L. C.; Chang-Chien, G. P. Polychlorinated dibenzo-*p*-dioxins/dibenzofuran mass distribution in both start-up and normal condition in the whole municipal solid waste incinerator. *J. Hazard. Mater.* **2008**, *160* (1), 37–44.

(8) Fiedler, H. Thermal formation of PCDD/PCDF: A survey. *Environ. Eng. Sci.* **1998**, *15* (1), 49–58.

(9) Froese, K. L.; Hutzinger, O. Polychlorinated benzene, phenol, dibenzo-*p*-dioxin, and dibenzofuran in heterogeneous combustion reactions of acetylene. *Environ. Sci. Technol.* **1996**, *30* (3), 998–1008.

(10) Khachatryan, L.; Burcat, A.; Dellinger, B. An elementary reaction-kinetic model for the gas-phase formation of 1,3,6,8- and 1,3,7,9-tetrachlorinated dibenzo-*p*-dioxins from 2,4,6-trichlorophenol. *Combust. Flame* **2003**, *132* (3), 406–421.

(11) Shaub, W. M.; Tsang, W. Dioxin formation in incinerators. *Environ. Sci. Technol.* **1983**, *17* (12), 721–730.

(12) Khachatryan, L.; Asatryan, R.; Dellinger, B. Development of expanded and core kinetic models for the gas phase formation of dioxins from chlorinated phenols. *Chemosphere* **2003**, *52* (4), 695–708.

(13) Evans, C. S.; Dellinger, B. Mechanisms of dioxin formation from the high-temperature oxidation of 2-chlorophenol. *Environ. Sci. Technol.* **2005**, *39* (1), 122–127.

(14) Huang, H.; Buekens, A. Comparison of dioxin formation levels in laboratory gas-phase flow reactors with those calculated using the Shaub−Tsang mechanism. *Chemosphere* **1999**, *38* (7), 1595–1602.

(15) Babushok, V.; Tsang, W. *Origins, Fate, and Health Effects*; 7th International Congress on Combustion By-Products; MBD, Inc.: Research Triangle Park, NC, 2001.

(16) Zhang, Q. Z.; Li, S. L.; Qu, X. H.; Wang, W. X. A quantum mechanical study on the formation of PCDD/Fs from 2-chlorophenol as precursor. *Environ. Sci. Technol.* **2008**, *42* (19), 7301–7308.

(17) Sidhu, S.; Edwards, P. Role of phenoxy radicals in PCDD/F formation. *Int. J. Chem. Kinet.* **2002**, *34* (9), 531–541.

(18) Weber, R.; Hagenmaier, H. PCDD/PCDF formation in fluidized bed incineration. *Chemosphere* **1999**, *38* (11), 2643–2654.

(19) Angerer, J.; Heinzow, B.; Reimann, D. O.; Knorz, W.; Lehnert, G. Internal exposure to organic substances in a municipal waste incinerator. *Int. Arch. Occup. Environ. Health* **1992**, *64* (4), 265–273.

(20) Kimbrough, R. D. Toxicity of chlorinated hydrocarbons and related compounds: Review including chlorinated dibenzodioxins and chlorinated dibenzofurans. *Arch. Environ. Health* **1972**, *25* (2), 125–131.

(21) Okamoto, Y.; Tomonari, M. Formation pathways from 2,4,5-trichlorophenol to polychlorinated dibenzo-*p*-dioxins (PCDDs): An ab initio study. *J. Phys. Chem. A* **1999**, *103* (38), 7686–7691.

(22) Frisch, M. J.; Trucks, G. W.; Schlegel, H. B.; Gill, P. W. M.; Johnson, B. G.; Robb, M. A.; Cheeseman, J. R.; Keith, T. A.; Petersson, G. A.; Montgomery, J. A.; Raghavachari, K.; Allaham, M. A.; Zakrzewski, V. G.; Ortiz, J. V.; Foresman, J. B.; Cioslowski, J.; Stefanov, B. B.; Nanayakkara, A.; Challacombe, M.; Peng, C. Y.; Ayala, P. Y.; Chen, W.; Wong, M. W.; Andres, J. L.; Replogle, E. S.; Gomperts, R.; Martin, R. L.; Fox, D. J.; Binkley, J. S.; Defrees, D. J.; Baker, J.; Stewart, J. P.; Head-Gordon, M.; Gonzales, C.; Pople, J. A. *Gaussian 03*; Gaussian, Inc.: Wallingford, CT, 2003.

(23) Zhao, Y.; Truhlar, D. G. Hybrid meta density functional theory methods for thermochemistry, thermochemical kinetics, and

noncovalent interactions: The MPW1B95 and MPWB1K models and comparative assessments for hydrogen bonding and van der Waals interactions. *J. Phys. Chem. A* **2004**, *108* (33), 6908–6918.
(24) Steckler, R.; Chuang, Y. Y.; Fast, P. L.; Corchade, J. C.; Coitino, E. L.; Hu, W. P.; Lynch, G. C.; Nguyen, K.; Jackells, C. F.; Gu, M. Z.; Rossi, I.; Clayton, S.; Melissas, V.; Garrett, B. C.; Isaacson, A. D.; Truhlar, D. G. *POLYRATE*, version 9.3; University of Minnesota: Minneapolis, MN, 2002.
(25) Baldridge, M. S.; Gordor, R.; Steckler, R.; Truhlar, D. G. Ab initio reaction paths and direct dynamics calculations. *J. Phys. Chem.* **1989**, *93* (13), 5107–5119.
(26) Gonzalez-Lafont, A.; Truong, T. N.; Truhlar, D. G. Interpolated variational transition state theory: Practical methods for estimating variational transition state properties and tunneling contributions to chemical reaction rates from electronic structure calculations. *J. Chem. Phys.* **1991**, *95* (12), 8875–8894.
(27) Garrett, B. C.; Truhlar, D. G. Generalized transition state theory. Classical mechanical theory and applications to collinear reactions of hydrogen molecules. *J. Phys. Chem.* **1979**, *83* (8), 1052–1079.
(28) Fernandez-Ramos, A.; Ellingson, B. A.; Garret, B. C.; Truhlar, D. G. Variational Transition State Theory with Multidimensional Tunneling. In *Reviews in Computational Chemistry*; Lipkowitz, K. B., Cundari, T. R. Eds; Wiley-VCH: Hoboken, NJ, 2007.
(29) Garrett, B. C.; Truhlar, D. G.; Wagner, A. F.; Dunning, T. H., Jr. Variational transition state theory and tunneling for a heavy-light-heavy reaction using an ab initio potential energy surface. ^{37}Cl+H(D) ^{35}Cl→H(D) ^{37}Cl+^{35}Cl. *J. Chem. Phys.* **1983**, *78* (7), 4400–4413.
(30) Skodje, R. T.; Truhlar, D. G.; Garrett, B. C. Vibrationally adiabatic models for reactive tunneling. *J. Chem. Phys.* **1982**, *77* (12), 5955–5976.
(31) Zhang, Q. Z.; Wang, S. K.; Gu, Y. S. A theoretical investigation on the mechanism and kinetics for the reaction of atomic O (^{3}P) with CH_3CHCl_2. *J. Chem. Phys.* **2003**, *119* (21), 11172–11179.
(32) Zhang, Q. Z.; Wang, S. K.; Zhou, J. H.; Gu, Y. S. Ab initio and kinetic calculation for the abstraction reaction of atomic O (^{3}P) with SiH_4. *J. Phys. Chem. A* **2002**, *106* (1), 115–121.
(33) Hellwege, K. H.; Hellwege A. M., Eds. Structure Data of Free Polyatomic Molecules. *Landolt-Bornstein*; Group II, Atomic and Molecular Physics; Springer-Verlag: Berlin, Germany, 1976; Volume *7*.
(34) Roussy, G.; Michel, F. Spectres de rotation de la molécule de chlorobenzéne: I. Variétés isotopiques monosubstituées et structure r_s. *J. Mol. Struct.* **1976**, *30* (2), 399–407.
(35) Boer, F. P.; Neuman, M. A.; Van Remoortere, F. P.; North, P. P.; Rinn, H. W. *Adv. Chem. Ser.* **1973**, *120*, 1.
(36) Grainger, J.; Reddy, V. V.; Patterson, D. G., Jr. Molecular geometry/toxicity correlations for laterally tetrachlorinated dibenzo-*p*-dioxins by Fourier transform infrared spectroscopy. *Chemospere* **1989**, *18* (1−6), 981.
(37) Mallard, W. G., Ed. National Institute of Standards and Technology (NIST) Chemistry Web Book: NIST Standard Reference; National Institute of Standards and Technology: Gaithersburg, MD, Database 69, 1998.
(38) Altarawneh, M.; Dlugogorski, B. Z.; Kennedy, E. M.; Mackie, J. C. Quantum chemical investigation of formation of polychlorodibenzo-*p*-dioxins and dibenzofurans from oxidation and pyrolysis of 2-chlorophenol. *J. Phys. Chem. A* **2007**, *111* (13), 2563–2573.
(39) Evans, C. S.; Dellinger, B. Mechanisms of dioxin formation from the high-temperature pyrolysis of 2-chlorophenol. *Environ. Sci. Technol.* **2003**, *37* (7), 1325–1330.
(40) Mulholland, J. A.; Akki, U.; Yang, Y.; Ryu, J. Y. Temperature dependence of DCDD/F isomer distributions from chlorophenol precursors. *Chemosphere* **2001**, *42* (5−7), 719–727.
(41) Ryu, J. Y.; Mulholland, J. A.; Kim, D. H.; Takeuchi, M. Homologue and isomer patterns of polychlorinated dibenzo-*p*-dioxins and dibenzofurans from phenol precursors: comparison with municipal waste incinerator data. *Environ. Sci. Technol.* **2005**, *39* (12), 4398–4406.
(42) Wu, Y. L.; Lin, L. F.; Hsieh, L. T.; Wang, L. C.; Chang-Chien, G. P. Atmospheric dry deposition of polychlorinated dibenzo-*p*-dioxins and dibenzofurans in the vicinity of municipal solid waste incinerators. *J. Hazard. Mater.* **2009**, *162* (1), 521–529.
(43) Melissas, V. S.; Truhlar, D. G. Interpolated variational transition state theory and tunneling calculations of the rate constant of the reaction OH + CH_4 at 223−2400 K. *J. Chem. Phys.* **1993**, *99* (2), 1013–1027.
(44) Baulch, D. L.; Cobos, C. J.; Cox, R. A.; Esser, C.; Frank, P.; Just, Th.; Kerr, J. A.; Pilling, M. J.; Troe, J.; Walker, R. W.; Warnatz, J. Evaluated kinetic data for combustion modeling. *J. Phys. Chem. Ref. Data* **1992**, *21* (3), 411–429.
(45) He, Y. Z.; Mallard, W. G.; Tsang, W. Kinetics of hydrogen and hydroxyl radical attack on phenol at high temperatures. *J. Phys. Chem.* **1988**, *92* (8), 2196–2201.
(46) Platz, J.; Nielsen, O. J.; Wallington, T. J.; Ball, J. C.; Hurley, M. D.; Straccia, A. M.; Schneider, W. F.; Sehested, J. Atmospheric chemistry of the phenoxy radical, C_6H_5O: UV spectrum and kinetics of its reaction with NO, NO_2, and O_2. *J. Phys. Chem. A* **1998**, *102* (41), 7964–7974.
(47) Zhang, Q. Z.; Qu, X. H.; Xu F.; Shi X. Y.; Wang, W. X. Mechanism and thermal rate constants for the complete series reactions of chlorophenols with H. *Environ. Sci. Technol.* **2009**, in press.

ES802835E